eJSSNT Regular Paper

e-Journal of Surface Science and Nanotechnology **20**, 25–30 (2022)

# CuPc Adsorption on Au(110)-(1 × 2): From a Monomer to a Periodic Chain

H. Koshida,† Y. Takahashi, H. Okuyama,‡ S. Hatta, T. Aruga

*Department of Chemistry, Graduate School of Science, Kyoto University, Kyoto 606-8502, Japan*
*†Present address: Institute of Industrial Science, The University of Tokyo, Komaba Meguro-ku, Tokyo 153-8505, Japan*
*‡Corresponding author: hokuyama@kuchem.kyoto-u.ac.jp*

Received: 31 January, 2022; Accepted: 10 February, 2022; J-STAGE Advance Publication: 17 March, 2022; Published: 17 March, 2022

Using scanning tunneling microscopy (STM), we study the adsorption of copper-phthalocyanine (CuPc) on the anisotropic Au(110)-(1 × 2) surface as a function of coverage. For the initial adsorption at room temperature, we observe CuPc monomers as well as a molecular chain that forms along the step edge. By STM manipulation, we reveal that the CuPc adsorption is accompanied by surface reconstruction from the initial adsorption stage; the periodicity beneath the monomer and the chain changes locally from (1 × 2) to (1 × 1) and (1 × 3), respectively. This finding highlights that the Au atom mobility of the surface plays an essential role in CuPc adsorption. At higher coverage, we observe the development of CuPc chains along the [1$\bar{1}$0] direction on the terrace with periodicities of (7 × 5) and (5 × 5), and compare the obtained results with those from the previous studies by diffraction methods.

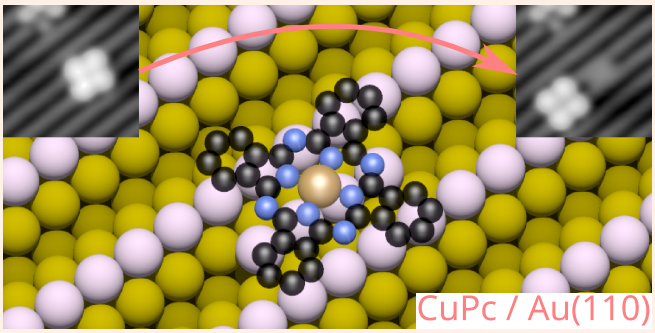


Keywords *Scanning tunneling microscopy; CuPc; Au(110); Surface reconstruction*

## I. INTRODUCTION

$\pi$-conjugated organic molecules have received much attention for their application in inexpensive, flexible, and tunable organic-based electronic and optoelectronic devices [1, 2]. Metal phthalocyanine (MPc) is a $\pi$-conjugated molecule composed of four pyrrole rings and four benzene rings, and contains a metal atom at the center of the unit [3]. MPcs are promising molecules for application in devices such as organic field-effect transistors (OFETs) and organic light-emitting diodes (OLEDs) because of their charge delocalization, high electron mobility, and tunability of electric properties by changing the metal atom [4, 5]. They are often used as thin films on surfaces for such applications. Thus, the "assembled" molecular structure is considered significant because the structure affects the electronic properties through some factors, such as the energy-level alignment, hybridization, and the formation of the electronic band structure from molecular orbitals. Owing to the rigid and planar structure of MPc with a high symmetry ($D_{4h}$), the molecules can form a periodic structure on many kinds of surfaces, and the correlation between the structure and electronic properties has been investigated [6, 7]. Notably, a long-range ordered assembly of MPcs can be produced using an anisotropic (patterned) substrate like a face-centered-cubic (110) surface [7]. Au(110) is typical for such a surface; a clean Au(110) surface displays a (1 × 2) reconstruction, where every second atomic row along [1$\bar{1}$0] lacks and forms a well-patterned trough across the [001] direction (called the "missing row structure") [8]. The adsorption structure of MPc on Au(110)-(1 × 2) has been extensively studied for MnPc [9, 10], FePc [11–16], CoPc [11, 16], CuPc [16–21], and $H_2$Pc [22, 23], mainly by low-energy electron diffraction (LEED) and STM. In the previous study, it has been revealed that MPcs form a well-ordered one-dimensional "chain" structure along the [1$\bar{1}$0] direction on Au(110), which implies that the anisotropy of the substrate has a significant effect on the assembled structure.

It has been well-known that the formation of the MPc chain is usually accompanied by the reconstruction of the Au(110)-(1 × 2) surface. For example, studies by LEED and helium atom scattering (HAS) showed that as the CuPc deposition increases, the diffraction spots due to (1 × 2) Au rows disappear. Instead, spots from higher-order periodicities

(×5, ×7, and ×3) appear along the [001] direction [17–19]. These studies indicate that large-scale Au row reconstruction contributes to chain formation. However, microscopic information about the adsorption process, which is essential for understanding the mechanism of the chain formation, remains lacking. Hence, local observation of the surface from the initial adsorption stage is necessary for further investigation. In addition, real-space observation studies of CuPc on surfaces are scarce [24], compared with those of other MPc molecules [10, 13–16, 22–24], which has hampered the understanding of CuPc adsorption.

In this study, we used STM to investigate the CuPc adsorption on Au(110)-(1 × 2), from the initial (monomeric) adsorption to chain formation. We employed an STM manipulation technique [25], which enabled us to move CuPc molecules and facilitate evaluation of the local structure at CuPc/Au(110) interface. We found that surface reconstruction commences under CuPc even at the initial adsorption stage, i.e., monomeric adsorption. In addition, we identified two CuPc chains on Au(110) that developed at higher coverage, confirmed the reconstruction of the substrate, and explained the correlation between the structure in real space and those in previous studies by diffraction methods.

## II. EXPERIMENTAL

All experiments were conducted in an ultrahigh vacuum (UHV) chamber equipped with STM (USM1200, Unisoku) at 4.5 K or 80 K. The single crystalline Au(110) surface was cleaned by repeated cycles of argon ion sputtering and annealing. The clean Au(110) surface exhibited the well-known missing-row reconstruction [8], and the (1 × 2) atomic-row structure was routinely observed in the STM images as straight lines running along the [1$\bar{1}$0] direction. CuPc molecules were deposited onto the room-temperature clean Au(110) surface by heating the crucible to 610 K. The coverage was controlled by the deposition time. The STM images were acquired in the constant current mode with an electrochemically etched tungsten tip as a probe. The STM images in this paper were slightly Gaussian-filtered to remove noise. We manipulated the CuPc molecule by STM as follows: we fixed the tip on the molecule, decreased the tip-molecule distance with the feedback loop open, and finally scanned the tip in a specific direction. We usually observed a current jump while decreasing the tip-molecule distance, which corresponded to molecular junction formation and was necessary for the manipulation [26–28].

## III. RESULTS AND DISCUSSION

### A. Initial adsorption of CuPc on Au(110)-(1 × 2)

Figure 1(a) shows a typical STM image of Au(110)-(1 × 2), onto which CuPc was deposited for 5 min. After the deposition, the sample was cooled to 80 K in approximately 30 min. The molecules were classified into three

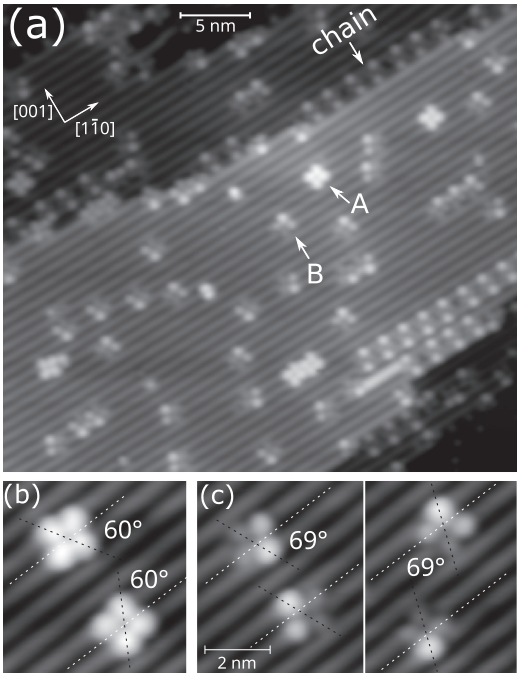


Figure 1: (a) Typical STM image of the Au(110)-(1 × 2) surface under initial exposure to CuPc vapor. The straight lines along [1$\bar{1}$0] are the missing rows of Au. Two types of monomers (denoted as *A* and *B*) and CuPc chains are observed. (b) Two equivalent orientations of *A*–CuPc. (c) Four orientations of *B*–CuPc. The angles between [1$\bar{1}$0] and the diagonal line of CuPc were 60° and 69° for *A*–CuPc and *B*–CuPc, respectively. The images were obtained at $V_s$ = 200 mV and $I$ = 1 nA.

types: two types of monomers [denoted as A and B in Figure 1(a)] and a chain [indicated in the upper right image in Figure 1(a)]. *A*–CuPc and *B*–CuPc show two and four different but equivalent configurations, respectively [Figure 1(b, c)], which reflects the $C_{2v}$ symmetry of the Au(110) surface. *A*–CuPc is imaged as a four-lobed leaf, which is in line with previous observations of the CuPc monomer on other surfaces, and mainly reflects the frontier orbitals ($2e_g$ and $1a_u$) localized in the organic ligand. On the other hand, *B*–CuPc shows four protrusions with different apparent heights. This suggests that *B*–CuPc adsorbs in a tilted manner, whereas *A*–CuPc is parallel to the surface.

In order to reveal the correlation between the STM images and the adsorption structure of CuPc, we investigated the interface below monomers (A, B) and chain by STM manipulation. Figures 2(a, b) show the sequential STM images of *A*–CuPc before and after STM manipulation along the yellow arrows, respectively. The trough where *A*–CuPc was originally placed appears "bright" in Figure 2(b). Figure 2(c, d) shows the STM manipulation process for *B*–CuPc. Contrary to *A*–CuPc, the site where *B*–CuPc was adsorbed appears "dark" [Figure 2(d)], indicating that the atomic row is partially lacking underneath *B*–CuPc. These results suggest that the Au(110)-(1 × 2) surface is reconstructed below the molecules.

Next, we obtained atomic-resolution STM images for the "bright" and "dark" regions, where the molecules adsorbed

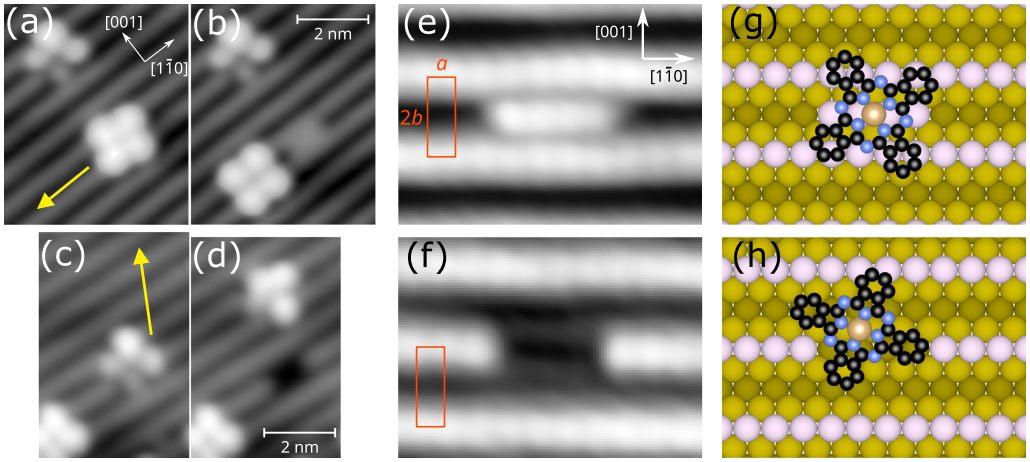


Figure 2: (a–d) STM manipulation processes for the CuPc monomer. By the manipulation of (a) *A*–CuPc [(c) *B*–CuPc], the molecule left a "bright" ["dark"] site under the molecule, as shown in (b) [(d)]. The atomic-resolution images (e, f) reveal that the "bright" area consists of four Au adatoms, whereas the "dark" area is devoid of Au atoms. The rectangle represents the Au(110)-(1 × 2) unit cell ($a$ = 0.29 nm, $b$ = 0.41 nm) (g, h) Schematics of *A*–CuPc and *B*–CuPc on the locally reconstructed Au(110) surface. The images were obtained at (a–d) $V_s$ = 200 mV and $I$ = 1 nA and (e, f) $V_s$ = 10 mV and $I$ = 1 nA.

[Figure 2(e, f)]. The atomic-resolution images were obtained at much lower junction resistance ($V_s$ = 10 mV and $I$ = 1 nA). The STM image of the "bright" region [Figure 2(e)] shows four protrusions, likely derived from Au adatoms, which form (1 × 1) structures together with the atoms of the nearby rows. This observation indicates that the (1 × 2) structure is lifted to the (1 × 1) structure by *A*–CuPc adsorption. We schematically illustrate the adsorption structure for *A*–CuPc in Figure 2(g), where the trough is locally filled with four Au adatoms, onto which the molecule adsorbs. Note that the number of Au adatoms was typically four but distributed between two to six, as we reported previously [25]. Figure 2(f) shows the atomic-resolution STM image of the "dark" area. Two rows are faintly visible in the "dark" area, and the distance between them is ~$b$ ($b = \sqrt{2}a$ = 0.41 nm, $a$ = 0.29 nm), which corresponds to the (1 × 1) rows distance along [001]. Hence, we suggest that the two rows are derived from the second layer of Au(110)-(1 × 2), and were observed due to the partial removal of Au atoms from the first layer. Thus, it follows that the substrate underneath *B*–CuPc also changed to a (1 × 1) structure, as illustrated in Figure 2(h). We suppose that *B*–CuPc partially fits into the (1 × 1) area [Figure 2(h)], which is likely responsible for the apparent-height difference of the four protrusions in the STM images.

Figure 3(a) shows an enlarged STM image of the CuPc chain along the step edge. Each molecule was imaged as a pair of bright protrusions with two smaller protrusions, as illustrated by the red circles in Figure 3(a). The diagonal line of CuPc was slightly offset from the [001] direction (~±10°). We also employed molecular manipulation to examine the interface below the chain, as shown in Figure 3(a–c). The distance between the atomic rows underneath the chain is more extended than 2$b$. We extracted the line profile in the [00$\bar{1}$] direction [along the red line in Figure 3(c)], which is shown as a red curve in Figure 3(d). The profile shows oscillation from the atomic rows, where the peak-to-peak distances are equal to 2$b$. In contrast, the interval below the chain is equal to 3$b$. This indicates that the distance between the Au rows along [001] changes from 2$b$ to 3$b$ below the chain, which is illustrated on the top of Figure 3(d). The possible reconstruction process is schematically depicted in Figure 3(e). The top of Figure 3(e) shows the Au(110)-(1 × 2) surface structure near the step before CuPc adsorption. When the molecule adsorbs, the outermost Au row, which is the closest to the step edge, moves in the [00$\bar{1}$] direction. Consequently, the (1 × 3) structure is locally formed, as shown in the bottom of Figure 3(e), and the molecules adsorb onto there. We will refer to this chain structure as "$\alpha$ chain" hereafter. Note that similar chains on the Au(110) terrace have been observed for MnPc [10] and $H_2$Pc [22, 23] using STM. We found that $\alpha$ CuPc chains are formed preferentially at the step edge. This probably originates from the mobility of Au atoms near the step edge.

The results presented here indicate that surface reconstruction occurs from the initial CuPc adsorption stage. We assume that such a surface reconstruction is inherent in the system of $\pi$-conjugated planar molecules (e.g., CuPc) on "corrugated" surfaces [e.g., Au(110)-(1 × 2)]; the molecule binds to the surface via the electronic coupling between the organic ligand (isoindole rings) and substrate [7, 25, 29]. Therefore, the molecule maximizes the contact area, i.e., the overlap between the molecular orbitals and surface electronic states. The (1 × 1) structure has a larger contact area than the (1 × 2) structure for flat molecules, and as shown in Ref. 22, the formation of the (1 × 3) structure also promotes hybridization between molecular orbitals and surface states. In addition, a DFT calculation study reported that the surface energy is very close from Au(110)-(1 × 1) to Au(110)-(1 × 6) with an energy minimum for Au(110)-(1 × 3) [30]. These are plausible reasons as to why CuPc adsorption readily induces the reconstruction of Au(110). The "adsorption with reconstruction" described above is primarily due to the facile

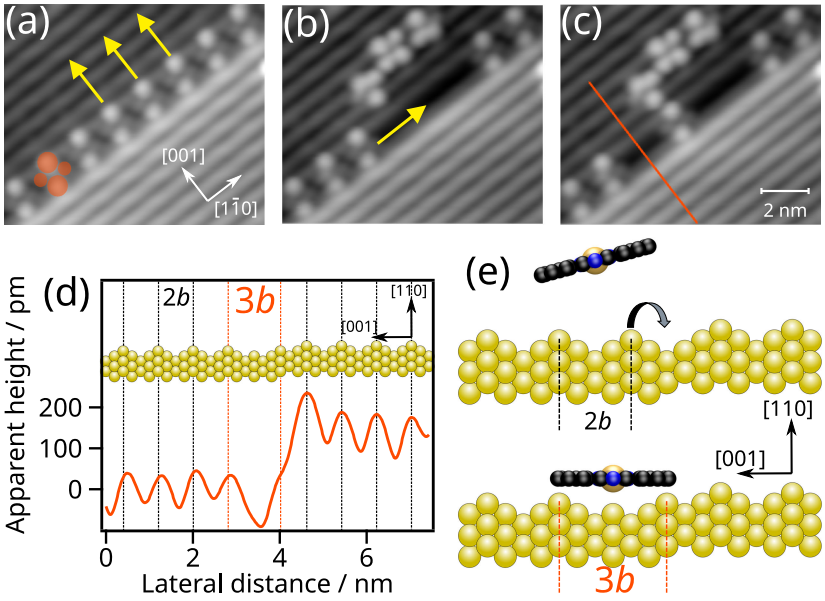


Figure 3: (a–c) STM manipulation processes for the CuPc chain grown along the step (yellow arrows). The molecular shape is represented in (a). (d) Apparent height along the red line in (c). The distance between the Au rows along [001] changes from 2*b* to 3*b* only where the molecules adsorb. The side view is also shown on the top. (e) Schematics of the (1 × 3) reconstruction at the step edge induced by CuPc adsorption. The images were obtained at $V_s = 200$ mV and $I = 1$ nA.

mobility of Au atoms on Au(110) surface. Similar phenomena have been reported in other organic molecules/coinage metal systems [31, 32]. We confirmed that the reconstruction was suppressed when the surface was exposed to CuPc at low temperatures (~100 K). This implies that the adsorption process accompanied by reconstruction is thermally activated and thus kinetically controlled.

## B. Development of CuPc chain on Au(110)-(1 × 2)

Figure 4(a) shows the STM image of Au(110)-(1 × 2) exposed to CuPc vapor for 7 min. Various structures, e.g., chains composed of *A*–CuPc and *B*–CuPc, are observed with increasing deposition time. We found that after the sample was kept at room temperature (RT), the molecules were activated thermally to form ordered structure. Figure 4(b) shows the STM image of Au(110)-(1 × 2) exposed to CuPc vapor for 5 min and kept at RT for 14 h. We can see that $\alpha$ chains also develop on the Au(110) terrace and instead, the monomers disappear, indicating that the $\alpha$ chain is thermally more stable than the monomers.

Figure 4(c) shows the STM image of Au(110)-(1 × 2) exposed to CuPc vapor for 10 min and kept at RT for 5 h. Most areas of the surface are covered with the $\alpha$ chain. Along with the $\alpha$ chain, we can find another type of CuPc chain indicated by the red arrow in Figure 4(c). This type of chain dominated the surface at higher coverage (exposure for 13 min), as shown in Figure 4(d). The chain is referred to as "$\beta$ chain" hereafter. Two types of molecular orientations in the $\beta$ chain were observed, as illustrated in Figure 4(d), and the orientation is aligned in each chain. The similar structure as $\beta$ chain has been observed in STM studies on MnPc [10] and FePc [13–15].

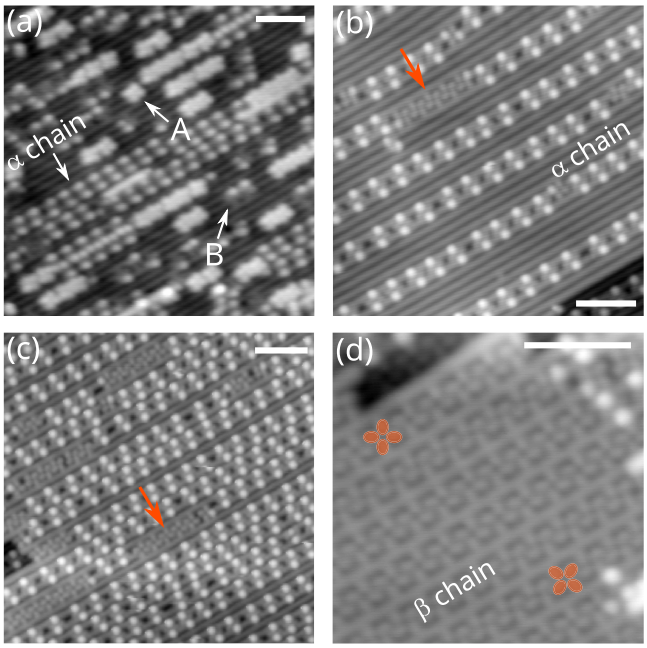


Figure 4: Growth of CuPc chains on the Au(110) surface. (a) STM images of the Au(110) exposed to CuPc for 7 min and immediately cooled to 80 K. *A*–CuPc, *B*–CuPc, as well as several disorder chains were observed. (b) STM images of the Au(110) exposed to CuPc for 5 min and kept at room temperature for 14 h. The molecules were arranged to form the $\alpha$ chain on the surface. (c, d) STM images of Au(110) exposed to CuPc for 10 min and 13 min, respectively (the samples were kept at room temperature for at least 5 h). As the coverage increases, the $\alpha$ chain and, subsequently, another chain ("$\beta$ chain") evolve on the surface. We note that the $\beta$ chains can be found at lower coverage, as shown by the red arrows in (b, c). The molecular shapes in the $\beta$ chain are drawn in (d). The scale bars represent 5 nm. The images were obtained at (a, c, d) $V_s = 500$ mV and $I = 1$ nA and (b) $V_s = 400$ mV and $I = 1$ nA.

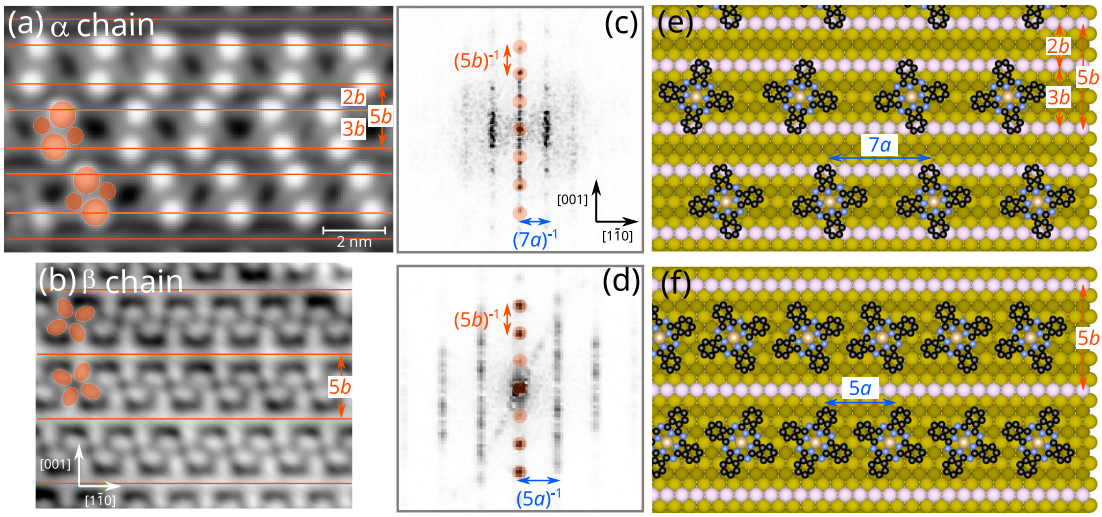


Figure 5: Enlarged STM images of (a) $\alpha$ and (b) $\beta$ chains. The surfaces of (a) and (b) were the same as those in Figure 4(c, d), respectively. The Au rows and molecular shapes are drawn in red. (c, d) Fourier transform of the same surfaces as (a) and (b), respectively. The spots of five-fold periodicity along [001] are shown by the red dots. Schematic structure of $\alpha$ and $\beta$ chains is shown in (e) and (f), respectively. The images were obtained at $V_s = 500$ mV and $I = 1$ nA. Size: $3.82 \times 3.82$ nm$^{-1}$ for (c) and (d).

Finally, we investigated the periodicity from the STM images of the chain. Figure 5(a, b) shows STM images of the $\alpha$ and $\beta$ chain cluster, and Figure 5(c, d) shows the 2D fast Fourier transform (FFT) of the same surface but for a larger area of Figure 5(a, b), respectively. The FFT pattern of the $\alpha$ [$\beta$] chain shows $(7 \times 5)$ [$(5 \times 5)$] periodicity and is streaked along the [001] direction, indicating that the positions of the molecules are not correlated between the chains [13, 14]. From the STM images and corresponding FFT patterns, we illustrate the schematic structure of $\alpha$ and $\beta$ chain cluster in Figure 5(e, f), respectively. For $\alpha$ chains [Figure 5(e)], the five-fold periodicity along [001] is realized by repeating $2b$ and $3b$, and the molecular distance along the [1$\bar{1}$0] direction is typically $7a$. For $\beta$ chains [Figure 5(f)], the interval of Au rows and molecules is equal to $5b$ and $5a$ along [001] and [1$\bar{1}$0], respectively, which is consistent with the $(5 \times 5)$ phase previously repotred [17–19]. Thus, it follows the CuPc molecules form the $(7 \times 5)$ phase consisting of $\alpha$ chains, followed by the $(5 \times 5)$ phase consisting of $\beta$ chains, in the early stage of chain formation. Note that previous diffraction studies have not reported such a $(7 \times 5)$ phase. This may be because of the relatively broad distributions of molecular intervals along the [1$\bar{1}$0] direction.

## IV. CONCLUSION

We studied the adsorption structure of CuPc on Au(110)-$(1 \times 2)$ and the surface reconstruction using STM. We found that CuPc adsorption is accompanied by surface reconstruction even in the monomeric adsorption regime; the structure beneath the monomer changes locally from $(1 \times 2)$ to $(1 \times 1)$. Besides, we identified two types of CuPc chains developed in higher coverage and revealed that the chains exhibit periodicities of $(7 \times 5)$ and $(5 \times 5)$ with surface reconstruction. This study suggests the importance of surface reconstruction for CuPc adsorption on a Au(110)-$(1 \times 2)$ surface.


### Acknowledgments

This work was supported by JSPS KAKENHI Grant Numbers 18K05030, 19J15306, and JST CREST Grant Number JPMJCR20R4, Japan.


### Note

This paper was presented at the 9th International Symposium on Surface Science (Online) from November 28 to December 1, 2021.

## References


[1] Y. Shirota, J. Mater. Chem. **10**, 1 (2000).
[2] A. Facchetti, Chem. Mater. **23**, 733 (2011).
[3] K. Kadish, K. M. Smith, and R. Guilard (Eds.), *The Porphyrin Handbook*, Vol. 3 (Elsevier, 2000).
[4] Z. Bao, A. J. Lovinger, and A. Dodabalapur, Appl. Phys. Lett. **69**, 3066 (1996).
[5] D. Hohnholz, S. Steinbrecher, and M. Hanack, J. Mol. Struct. **521**, 231 (2000).
[6] J. Otsuki, Coord. Chem. Rev. **254**, 2311 (2010).
[7] J. M. Gottfried, Surf. Sci. Rep. **70**, 259 (2015).
[8] G. Binnig, H. Rohrer, C. Gerber, and E. Weibel, Surf. Sci. **131**, L379 (1983).
[9] P. Gargiani, S. Lisi, G. Avvisati, P. Mondelli, S. Fatale, and M. G. Betti, J. Chem. Phys. **147**, 134702 (2017).
[10] M. Topyła, N. Néel, and J. Kröger, Langmuir **32**, 6843 (2016).
[11] M. G. Betti, P. Gargiani, R. Frisenda, R. Biagi, A. Cossaro, A. Verdini, L. Floreano, and C. Mariani, J. Phys. Chem. C **114**, 21638 (2010).
[12] M. G. Betti, P. Gargiani, C. Mariani, S. Turchini, N. Zema, S. Fortuna, A. Calzolari, and S. Fabris, J. Phys. Chem. C **116**, 8657

(2012).
[13] M. G. Betti, P. Gargiani, C. Mariani, R. Biagi, J. Fujii, G. Rossi, A. Resta, S. Fabris, S. Fortuna, X. Torrelles, M. Kumar, and M. Pedio, Langmuir **28**, 13232 (2012).
[14] S. Fortuna, P. Gargiani, M. G. Betti, C. Mariani, A. Calzolari, S. Modesti, and S. Fabris, J. Phys. Chem. C **116**, 6251 (2012).
[15] P. Gargiani, M. G. Betti, A. T. Ibrahimi, P. Le Fevre, and S. Modesti, J. Phys. Chem. C **120**, 28527 (2016).
[16] L. Massimi, M. Angelucci, P. Gargiani, M. G. Betti, S. Montoro, and C. Mariani, J. Chem. Phys. **140**, 244704 (2014).
[17] F. Evangelista, A. Ruocco, V. Corradini, M. Donzello, C. Mariani, and M. G. Betti, Surf. Sci. **531**, 123 (2003).
[18] A. Cossaro, D. Cvetko, G. Bavdek, L. Floreano, R. Gotter, A. Morgante, F. Evangelista, and A. Ruocco, J. Phys. Chem. B **108**, 14671 (2004).
[19] L. Floreano, A. Cossaro, R. Gotter, A. Verdini, G. Bavdek, F. Evangelista, A. Ruocco, A. Morgante, and D. Cvetko, J. Phys. Chem. C **112**, 10794 (2008).
[20] F. Evangelista, A. Ruocco, R. Gotter, A. Cossaro, L. Floreano, A. Morgante, F. Crispoldi, M. Betti, and C. Mariani, J. Chem. Phys. **131**, 174710 (2009).
[21] D. Lüftner, M. Milko, S. Huppmann, M. Scholz, N. Ngyuen, M. Wießner, A. Schöll, F. Reinert, and P. Puschnig, J. Electron Spectrosc. Relat. Phenom. **195**, 293 (2014).
[22] E. Rauls, W. Schmidt, T. Pertram, and K. Wandelt, Surf. Sci. **606**, 1120 (2012).
[23] T. Pertram, M. Moors, and K. Wandelt, J. Phys.: Condens. Matter **28**, 434001 (2016).
[24] P. Gargiani, G. Rossi, R. Biagi, V. Corradini, M. Pedio, S. Fortuna, A. Calzolari, S. Fabris, J. C. Cezar, N. Brookes, and M. G. Betti, Phys. Rev. B **87**, 165407 (2013).
[25] H. Koshida, H. Okuyama, S. Hatta, T. Aruga, Y. Hamamoto, I. Hamada, and Y. Morikawa, J. Phys. Chem. C **124**, 17696 (2020).
[26] Y. Kitaguchi, S. Habuka, H. Okuyama, S. Hatta, T. Aruga, T. Frederiksen, M. Paulsson, and H. Ueba, Beilstein J. Nanotechnol. **6**, 2088 (2015).
[27] Y. Kitaguchi, S. Habuka, H. Okuyama, S. Hatta, T. Aruga, T. Frederiksen, M. Paulsson, and H. Ueba, Sci. Rep. **5**, 11796 (2015).
[28] H. Okuyama, Y. Kitaguchi, T. Hattori, Y. Ueda, N. Ferrer, S. Hatta, and T. Aruga, J. Chem. Phys. **144**, 244703 (2016).
[29] Y. Huang, E. Wruss, D. Egger, S. Kera, N. Ueno, W. Saidi, T. Bucko, A. Wee, and E. Zojer, Molecules **19**, 2969 (2014).
[30] M. Landmann, E. Rauls, and W. Schmidt, Phys. Rev. B **79**, 045412 (2009).
[31] P. Maksymovych, O. Voznyy, D. B. Dougherty, D. C. Sorescu, and J. T. Yates Jr, Prog. Surf. Sci. **85**, 206 (2010).
[32] M. Schunack, L. Petersen, A. Kühnle, E. Lægsgaard, I. Stensgaard, I. Johannsen, and F. Besenbacher, Phys. Rev. Lett. **86**, 456 (2001).